Title

Biodistribution of the Multidentate Hydroxypyridinonate Ligand [14C]-3,4,3-LI(1,2-HOPO), a Potent Actinide Decorporation Agent

Journal

Drug Development Research, 76(3)

ISSN

0272-4391

Authors

Choi, Taylor A
Endsley, Aaron N
Bunin, Deborah I
et al.

Publication Date

2015-05-01

DOI

10.1002/ddr.21246

Peer reviewed

DRUG DEVELOPMENT RESEARCH 76 : 107–122 (2015)

DDR

Research Article

Biodistribution of the Multidentate Hydroxypyridinonate Ligand [^{14}C]-3,4,3-LI(1,2-HOPO), a Potent Actinide Decorporation Agent

Taylor A. Choi,[1] Aaron N. Endsley,[2] Deborah I. Bunin,[2] Christophe Colas,[2] Dahlia D. An,[1] Joel A. Morales-Rivera,[1] Jonathan A. Villalobos,[1] Walter M. Shinn,[2] Jack E. Dabbs,[2] Polly Y. Chang,[2] and Rebecca J. Abergel[1]*

[1]*Chemical Sciences Division, Lawrence Berkeley National Laboratory, Berkeley, CA, USA*
[2]*Biosciences Division, SRI International, Menlo Park, CA, USA*

Strategy, Management and Health Policy				
Enabling Technology, Genomics, Proteomics	Preclinical Research	Preclinical Development Toxicology, Formulation Drug Delivery, Pharmacokinetics	Clinical Development Phases I-III Regulatory, Quality, Manufacturing	Postmarketing Phase IV

ABSTRACT The pharmacokinetics and biodistribution of the ^{14}C-labeled actinide decorporation agent 3,4,3-LI(1,2-HOPO) were investigated in young adult Swiss Webster mice and Sprague Dawley rats, after intravenous, intraperitoneal, and oral dose administration. In all routes investigated, the radiolabeled compound was rapidly distributed to various tissues and organs of the body. In mice, the 24 h fecal elimination profiles suggested that the biliary route is the predominant route of elimination. In contrast, lower fecal excretion levels were observed in rats. Tissue uptake and retention of the compound did not differ significantly between sexes although some differences were observed in the excretion patterns over time. The male mice eliminated a greater percentage of ^{14}C through the renal pathway than the female mice after receiving an intravenous or intraperitoneal dose, while the opposite trend was seen in rats that received an intravenous dose. Metabolite profiling performed on selected rat samples demonstrated that a putative major metabolite of [^{14}C]-3,4,3-LI(1,2-HOPO) is formed, accounting for approximately 10% of an administered oral dose. Finally, to improve its oral bioavailability, 3,4,3-LI(1,2-HOPO) was coformulated with a proprietary permeability enhancer, leading to a notable increase in oral bioavailability of the compound. Drug Dev Res 76 : 107–122, 2015.

Key words: 3,4,3-LI(1,2-HOPO); actinide decorporation; biodistribution; pharmacokinetics; metabolite

INTRODUCTION

In the event of internal exposure of a large population to radionuclides such as actinide isotopes, logistical management of its consequences is imperative. One practical strategy is to have orally effective metal-chelating drugs stored in the US Strategic National Stockpile readily available for prompt distribution as the need arises. To date, the only US Food and Drug Administration- (FDA-) approved chelating agents available in the stockpile are calcium (Ca)- and zinc (Zn)-diethylenetriamine pentaacetic acid

Contract grant sponsor: National Institutes of Health/National Institute of Allergy and Infectious Diseases Medical Countermeasures Against Radiological Threats (MCART) Consortium; contract grant number: #HHSN272201000046C; Contract grant sponsor: US Department of Energy; contract grant number: #DE-AC02-05CH11231

*Correspondence to: Rebecca J. Abergel, Chemical Sciences Division, Lawrence Berkeley National Laboratory, 1 Cyclotron Road, Berkeley, CA 94720. E-mail: rjabergel@lbl.gov

Received 26 January 2015; Accepted 17 February 2015

Published online in Wiley Online Library (wileyonlinelibrary.com). DOI: 10.1002/ddr.21246

(DTPA) [US Food and Drug Administration, 2004; US Food and Drug Administration, 2006]. In the current approved formulations, administration of these two products is limited to intravenous or inhalational routes [Cassatt et al., 2008]. Furthermore, efficacy studies show that DTPA is only effective in decorporating americium (Am) and plutonium (Pu) but ineffective at chelating other actinides such as uranium (U) and neptunium (Np) [Cerveny 1989; Durbin 2006]. Therefore, safe and effective oral drugs that can stably form chelates with a wider spectrum of metal ions and are relevant to medical management of internal radionuclides are urgently needed.

Inspired by the coordination chemistry of naturally occurring siderophores, a class of hydroxypyridinone ligands was synthesized through structure-based metal-chelating design [Durbin et al., 2003; Gorden et al., 2003; Durbin 2008]. In particular, the octadentate ligand 3,4,3-LI(1,2-HOPO) (Fig. 1) has been identified as an effective metal chelator. This active pharmaceutical ingredient (API) is currently undergoing development as a prospective therapeutic actinide decorporation agent [Abergel et al., 2010; Jarvis et al., 2012; Bunin et al., 2013], and received an Investigational New Drug (IND) designation from the FDA in August 2014. When orally administered to rodents and dogs, 3,4,3-LI(1,2-HOPO) can sequester a wider spectrum of internally deposited radionuclides than DTPA [Durbin 2008; Abergel et al., 2010; Abergel and Raymond 2011]; it coordinates Pu, Am, U, and Np with high affinity and forms stable, excretable complexes at physiological pH [Durbin 2008; Kullgren et al., 2013]. Limited preclinical efficacy and safety profiles of this compound have been previously reported [Durbin 2008; Abergel et al., 2010], highlighting its high potency and relatively low toxicity in vivo. However, in order to seek regulatory approval of 3,4,3-LI(1,2-HOPO) as a new radionuclide decorporation agent, detailed pharmacology, toxicology, and efficacy assessments are needed [US Food and Drug Administration, 2009]. Herein, we report the tissue distribution of 3,4,3-LI(1,2-HOPO), labeled with ^{14}C, in healthy male and female mice and rats after a single dose administered by intravenous (iv), intraperitoneal (ip; mice only), or oral (po) route, using liquid scintillation counting (LSC) as the method of detection. Metabolite profiling of [^{14}C]-3,4,3-LI(1,2-HOPO) was then performed on selected urine, feces, kidney, liver, and lung samples from the administered rats. To improve the systemic availability of the orally delivered ligand, the API was coformulated with a proprietary permeability enhancer (PE). Comparative analysis of the bioavailability and excretion pattern of the API with or without PE was also conducted.

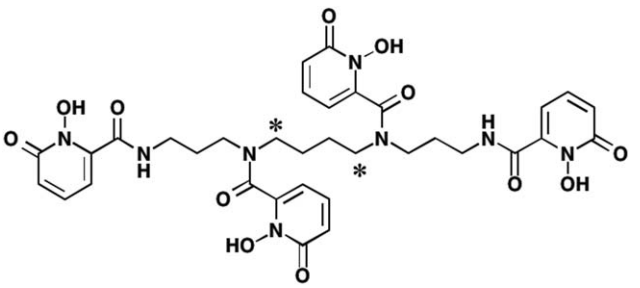

Fig. 1. Structure of the octadentate actinide chelator 3,4,3-LI(1,2-HOPO); the * indicate the ^{14}C labels.

MATERIALS AND METHODS

Materials

The parent compound 3,4,3-LI(1,2-HOPO) was synthesized and characterized by Ash Stevens, Inc. (Detroit, MI) as previously described [Abergel et al., 2010]. Purity was determined to be 98.5% by HPLC analysis (data not shown). The radiolabeled [^{14}C]-3,4,3-LI(1,2-HOPO) (specific radioactivity: 62.6 mCi/mmol, radiochemical purity: 98.7%; data not shown) was synthesized and characterized by Moravek Biochemicals, Inc. (Brea, CA). Two ^{14}C labels were inserted on the spermine backbone of 3,4,3-LI(1,2-HOPO), as shown in Figure 1. All other chemicals were obtained from commercial suppliers and used as received.

Preparation of Dose Formulations

Stock solutions of the radiolabeled component were prepared in sterile water (Baxter, Deerfield, IL), prior to being added to the dose formulations, in appropriate quantities. Formulations were prepared by dissolving the appropriate amount of API and [^{14}C]-3,4,3-LI(1,2-HOPO) in isotonic saline (Baxter, Deerfield, IL) for mouse studies or Dulbecco's phosphate buffered saline (PBS, Sigma-Aldrich, Milwaukee, WI) for rat studies. In some instances, this was followed by the addition of a proprietary PE (purity: >97.0%; TCI America, Portland, OR). The solution was then adjusted with 1 M NaOH to a final pH of 7.0 for parenteral formulations, 7.4 for mouse po formulations, and 6.5 for rat po formulations; parenteral solutions were filter-sterilized (0.2 μm). The final stable API concentrations and corresponding specific activities were as follows: 13 mg/mL (17.5 μCi/mL) for mouse iv, ip, and po formulations; 15 mg/mL (40

μCi/mL) and 7.5 mg/mL (20 μCi/mL) for rat iv and po formulations, respectively.

General Procedures for In Vivo Mouse Studies

All protocols were reviewed and approved by the Institutional Animal Care and Use Committee (IACUC) of Lawrence Berkeley National Laboratory, and were performed in Association for Assessment and Accreditation of Laboratory Animal Care International (AAALAC)-accredited facilities. Male and female Swiss Webster mice (11-12 weeks old; 31.7 ± 2.0 g and 29.8 ± 2.6 g, respectively) were purchased from Simonsen Laboratories (Gilroy, CA). Animals were kept under a 12-h light cycle with controlled temperature (20–25 °C) and relative humidity (30–70%), and were given food and water ad libitum. Mice were fasted 16 h prior to dose administration and their normal feeding schedule was resumed 2 hours after dosing. Under isoflurane anesthesia, mice ($n = 3$ per euthanasia group) received a single iv (into a warmed lateral tail-vein), ip, or po (via plastic gavage tube) dose of 100 μCi/kg [^{14}C]-3,4,3-LI(1,2-HOPO), except the male mice administered iv or ip doses received 50 μCi/kg [^{14}C]-3,4,3-LI(1,2-HOPO) (in pharmacokinetic evaluations, the dose for male mice administered iv and ip was normalized to account for half the dose administered to the female mice). Mice were group-housed ($n = 3$) in plastic metabolism cages (Tecniplast, Exton, PA), except for those groups that were bled and euthanized at $\leq$15 min postdose. At the scheduled times after dosing (iv and ip routes: 0.083, 0.25, 0.5, 1, 4, 24 h; po route: 0.5, 0.75, 1, 2, 6, 24 h), approximately 1 mL of blood was obtained via cardiac puncture from anesthetized mice and collected into K_2EDTA Microtainer® tubes (Becton Dickinson and Company, Franklin Lakes, NJ). Blood samples were centrifuged at 4,000 rpm for 15 min to obtain plasma. Harvested plasma was transferred to Nunc® cryovials (ThermoFisher Scientific, Waltham, MA) and stored at −80 °C until analysis. Pooled urine and pooled fecal samples were collected in polypropylene screw-cap tubes and stored at −80 °C until analysis. Mice were euthanized by cervical dislocation immediately after the scheduled blood collection and liver and kidneys were harvested. Organs were collected in Nunc® cryovials (ThermoFisher Scientific, Waltham, MA) and stored at −80 °C until analysis.

General Procedures for In Vivo Rat Studies

All protocols were reviewed and approved by the IACUC of Lawrence Berkeley National Laboratory and SRI International, and were performed in AAALAC-accredited facilities. This study was designed slightly differently from the mouse study for compound availability and scheduling reasons. Male and female Sprague Dawley rats (8-9 weeks and 9–10 weeks; 239–277 g and 183–207 g, respectively) were purchased from Charles River (Hollister, CA). Housing room and feed conditions were as described for the mice. Among those rats assigned to the experiments, nine of each sex were single jugular vein catheterized (JVC) by the vendor prior to shipment. Rats ($n = 3$ per euthanasia group) were administered a single iv (through the JVC) or po (via plastic gavage tube) dose of 200 μCi/kg [^{14}C]-3,4,3-LI(1,2-HOPO). Animals were group-housed in hanging polycarbonate cages (early euthanasia groups) or individually housed in custom-built glass metabolism cages (Crown Glass Co., Somerville, NJ). Blood (approximately 1 mL and 1.5 mL interim and terminal collections, respectively) was collected from the retro-orbital sinus under 60:40% CO_2:O_2 anesthesia into tubes containing K_3EDTA. Plasma samples were stored frozen at −80 °C. Pooled urine and pooled fecal samples were collected in plastic wide mouth bottles and stored at −80 °C until analysis. Immediately after the terminal blood collection, rats were euthanized by overdose of sodium pentobarbital administered ip before harvesting brain, kidneys liver, lungs, spleen, and skeletal muscle (from right hind quarter). Carcass and gastrointestinal (GI) tract (stomach, small intestine, and large intestine) were also processed from the rats sacrificed 24 h postdose. Tissues were stored at −80 °C until analysis.

Radioactivity Determination

Radioactivity was determined by LSC (Packard Tri-Carb model B4430 or 2900TR, Perkin Elmer Corporation, Shelton, CT), using the external standard method of correcting for counting efficiency. For liquid samples (urine, cage wash, and plasma), aliquots were mixed directly with scintillation cocktail and counted. Mouse fecal samples were diluted in water (1:6 w/v) and mechanically homogenized using a Tissue-Tearor (Biospec Products, Inc., Bartlesville, OK). Mouse liver and kidney samples were diluted in Hank's Balanced Salt Solution (1:3 w/v; Life Technologies, Grand Island, NY) before homogenization. The mixtures were centrifuged (8,000 rpm, 4 °C, 10 min) and aliquots of the supernatants were combined with Ultimagold® (Perkin Elmer Corporation, Waltham, MA) for LSC. Rat tissues and feces were physically homogenized in water using an IKA T25 digital Ultra-Turrax dispersion

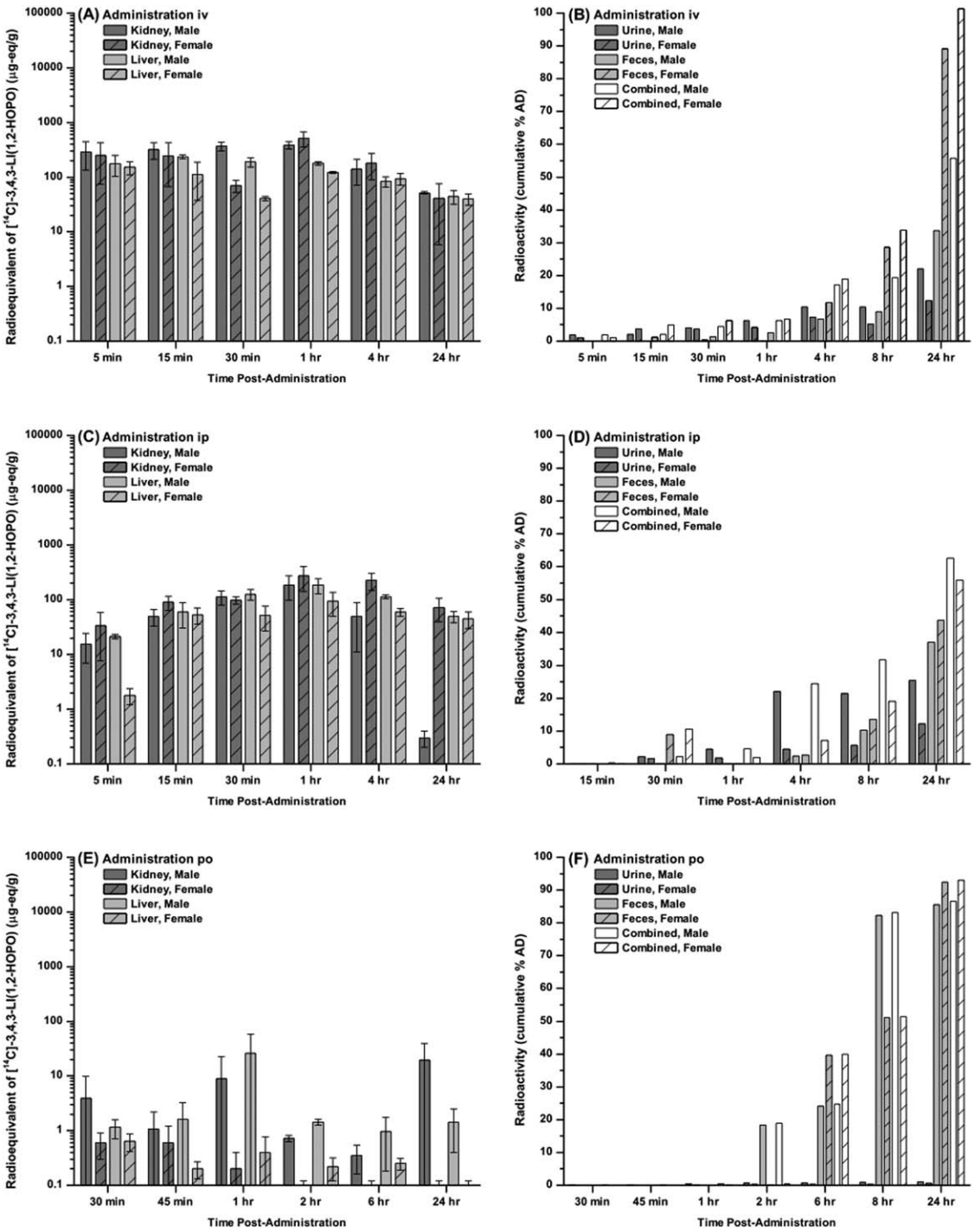

Fig. 2. Retention in the liver and kidneys (left, Panels A, C, and E) and excretion (right, Panels B, D, and F) of radioactivity from [^{14}C]-3,4,3-LI(1,2-HOPO) in male and female mice after iv (top, Panels A and B), ip (middle, Panels C and D), or po (bottom, Panels E and F) administration. Groups of mice ($n = 3$ per euthanasia group) were administered a single dose of [^{14}C]-3,4,3-LI(1,2-HOPO) and were euthanized at six time points from 5 min to 24 h postdose. Data expressed as μg-eq (mean $\pm$ SD) for tissue content and as percentage of administered dose (% AD) for excreta; excreta of each three-mouse group were pooled and standard deviations are not available.

tool (Sigma-Aldrich Corp., St. Louis, MO). Potassium hydroxide (2 M) in methanol was used to chemically solubilize the rat carcasses. Rat fecal, tissue, and carcass samples were combusted using a tissue oxidizer (Packard Instrument Company, Model 307, Meriden, CT); the radioactive carbon was

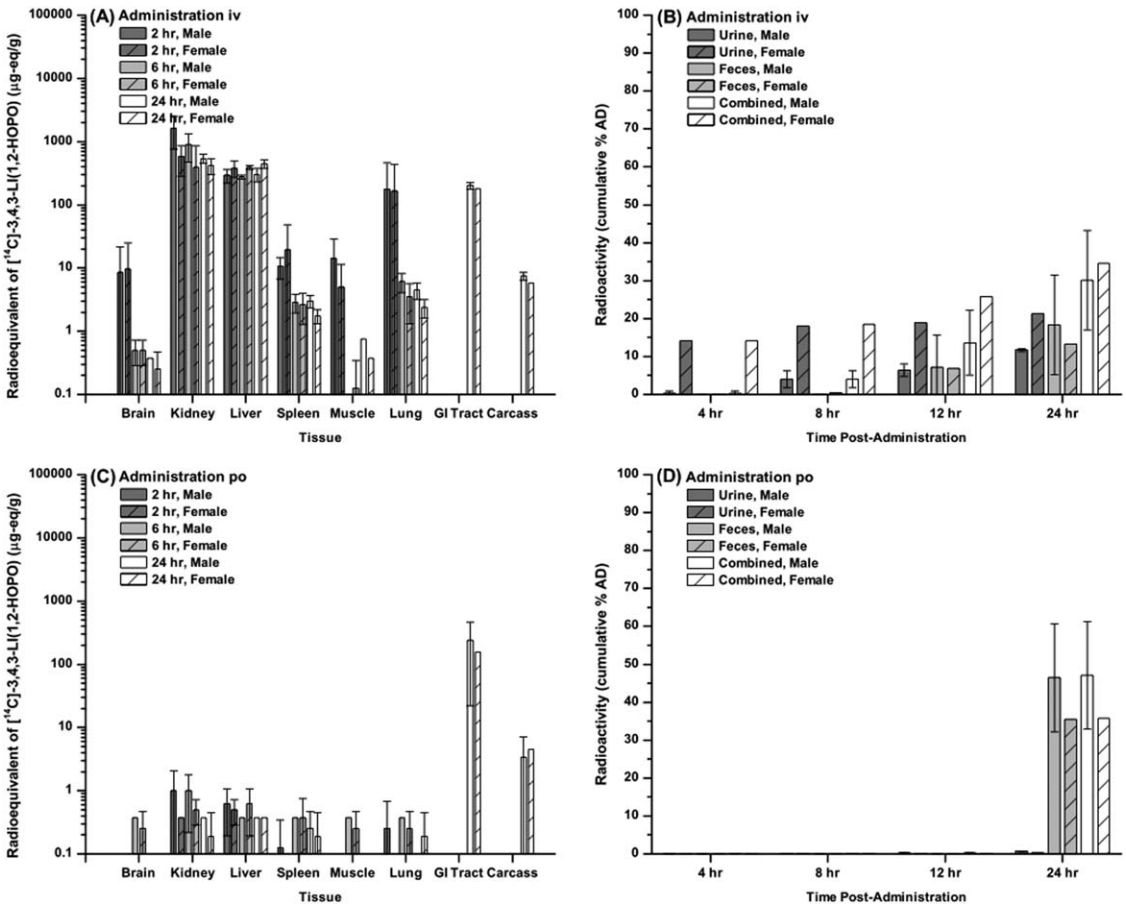

Fig. 3. Retention (left, Panels A and C) and excretion (right, Panels B and D) of radioactivity from [^{14}C]-3,4,3-LI(1,2-HOPO) in male and female rats after iv (top, Panels A and B) or po (bottom, Panels C and D) administration. Groups of rats ($n = 3$ per euthanasia group) were administered a single dose of [^{14}C]-3,4,3-LI(1,2-HOPO) and were euthanized at three time points between 2 h and 24 h postdose. Data expressed as μg-eq (mean ± SD) for tissue content and as percentage of administered dose (% AD; mean ± SD) for excreta.

collected in Carbo-Sorb E and mixed with Permafluor E for analysis of radioactivity by LSC. Duplicate aliquots were evaluated for each sample. Samples with greater than 100 dpm for which radioactivity (dpm/g of aliquot) in the duplicates varied more than 10% from the mean value were reanalyzed. The radioactivity in dpm was corrected for the weight of the aliquot analyzed and then corrected for total weight of the tissue to determine the total radioactivity in that tissue (μCi/g). Concentrations were calculated by converting total radioactivity in each tissue (μCi/g) to µg-equivalents (μg-eq) using the [^{14}C]-3,4,3-LI(1,2-HOPO) specific activity of the administered dose formulation. The calculated radioactivities in plasma and tissue samples (including carcass) were then reported as a concentration (µg-eq/mL of plasma or µg-eq/g of tissue), and as a percent of the administered dose (%AD). Material recoveries are not available since not all organs were processed for analysis.

Pharmacokinetic Analysis

The radioactivity concentration data in plasma was analyzed with Phoenix® WinNonlin® version 6.3 by noncompartmental modeling [Rowland and Tozer, 1995]. The following pharmacokinetic parameters were determined for plasma: radioactivity concentration at first blood sampling time (C_p) and concentration extrapolated to time 0 (C_0) after the iv dose, maximum radioactivity concentration (C_{max}) and time to maximum concentration (T_{max}) after the po dose, area under the concentration-time curve to the last time point (AUC_{last}), and elimination half-life ($t_{1/2}$). Statistical analyses were performed using GraphPad Prism Version 6.0d (GraphPad Software, Inc., San Diego, CA). The statistical significance of difference between male and female groups was evaluated by the *t*-test. Comparison of the pharmacokinetic parameters for routes of administration was performed using a two-way analysis of variance (ANOVA). Statistical significance was defined as $P < 0.05$.

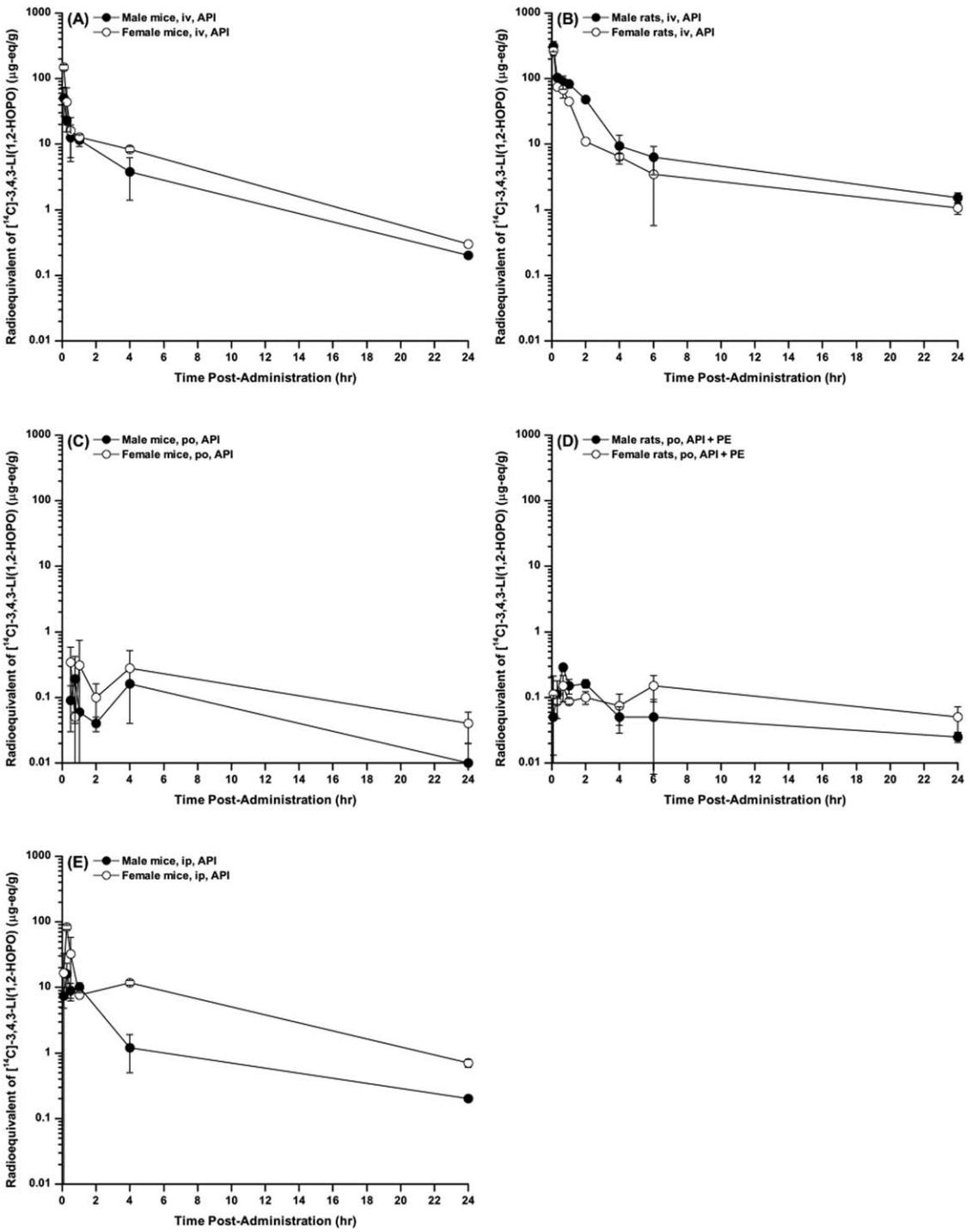

Fig. 4. Mean plasma time course ($n = 3$) of radioactivity from [^{14}C]-3,4,3-LI(1,2-HOPO) ± SD over 24 h in male and female mice after (A) iv, (C) po, or (E) ip administration and in male and female rats after (B) iv or (D) po administration.

Metabolite Profile Determination

Metabolite profile analysis was performed on plasma, urine, or homogenized specimens prepared for the tissue distribution portion of the rat studies. Samples selected for metabolite profiling were those containing the highest levels of radioactivity. Homogenates were rapidly thawed in a water bath at 37 °C, vortexed vigorously, and sonicated at room temperature (RT) for 5 min. A 360 μL aliquot of each was transferred into a plastic microcentrifuge tube, mixed

TABLE 1. Mean Pharmacokinetic Parameters of [^{14}C]-3,4,3-LI(1,2-HOPO) in Male and Female Swiss Webster Mice and Sprague Dawley Rats ($n = 3$)

Route	Species	Sex	Dose (μmol/kg)	C_0* or C_{max} (μg-eq/mL)	T_{max} (h)	AUC** (h μg-eq/mL)	$t_{1/2}$ (h)	F† (%)
iv	Mouse	M	50	76 ± 47	NA††	41.7 ± 3.2	1.6 ± 0.5	NA
		F	100	342 ± 211	NA	162 ± 21.5	1.6 ± 0.3	NA
	Rat	M	100	463	NA	354 ± 26.9	8.1	NA
		F	100	422	NA	211 ± 28.7	8.6	NA
ip	Mouse	M	50	16.4 ± 7.1	0.33 ± 0.14	39.8 ± 10.5	NA	NA
		F	100	61.7 ± 36.7	0.33 ± 0.14	188 ± 14.0	NA	NA
po	Mouse	M	100	0.32 ± 0.23	0.63 ± 0.18	1.94 ± 2.80	NC‡	1.2
		F	100	0.55 ± 0.29	0.67 ± 0.29	3.93 ± 3.17	NC	2.6
	Rat	M	100	0.29 ± 0.20	0.67	1.30 ± 0.37	NC	0.4
		F	100	0.15 ± 0.04	0.68	2.40 ± 0.44	NC	1.2

*C_0 is the plasma concentration extrapolated to time zero.
**AUC presented is calculated to the last data point at 24 h.
†The bioavailability F is calculated using the formula: $[(Dose_{iv} \times AUC_{po})/(Dose_{po} \times AUC_{iv})] \times 100\%$
††NA = not applicable.
‡NC = not calculated; insufficient data for parameter estimation.

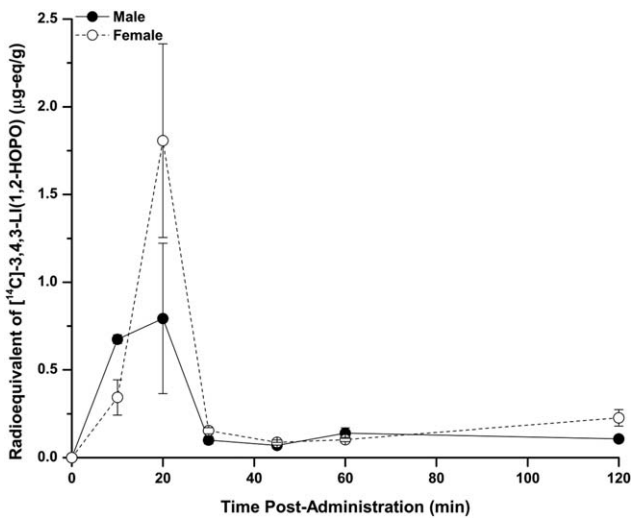

Fig. 5. Mean plasma time course ($n = 3$) of radioactivity from [^{14}C]-3,4,3-LI(1,2-HOPO) over 2 h in male and female mice after po administration of the co-formulated API with PE.

with 45 μL of an aqueous solution containing 20% acetic acid, 500 mM ammonium acetate and 100 mM EDTA, and supplemented with 45 μL of methanol. The resulting samples were sonicated (RT, 5 min) and centrifuged (RT, 18,000 × *g*, 5 min). Supernatants were transferred to new plastic microcentrifuge tubes and stored at −80 °C. Upon thawing, samples were centrifuged (RT, 18,000 × *g*, 5 min), with the resulting supernatants transferred into High Performance Liquid Chromatography (HPLC) vials fitted with deactivated glass inserts for analysis. Matrix controls were prepared similarly, by spiking 360 μL aliquots of select samples of urine, feces, kidney, and liver with 2 μL of the iv group dosing solution. Samples were assayed in duplicate on a Waters 2695 Alliance Integrated HPLC System following an analytical method shown to yield only one peak upon injection of an aliquot of [^{14}C]-3,4,3-LI(1,2-HOPO) over a concentration range of 6 to 200 μM. Chromatographic separation was achieved on a Gemini C18 column (Phenomenex, Torrance, CA, USA; 3 μm, 2 × 150 mm) fitted with guard column and maintained at 40 °C with two mobile phases containing 20 mM ammonium acetate, 2 mM EDTA, and 0.2% acetic acid [(A) 10% (v:v) methanol in water and (B) 20% (v:v) water in methanol]. Samples (50 μL) were eluted using a gradient from 0% B to 45% B over 27 min. The flow rate was maintained at 0.3 mL/min. Analytes were detected by a LabLogic βRAM-4 In-line Flow Scintillation Counter (150 μL cell volume, 1.2 mL/min cocktail flow rate) with Flowlogic™ U scintillation cocktail (LabLogic, Brandon, FL). All chromatograms were found to have at least one peak above background. For each sample, the areas of the identified peaks were measured using the Laura 4.1.10 software (Lablogic) and are reported as a percentage of the sum of all peak areas for each radiochromatogram. Due to normal variations in retention times between samples, retention time ranges (rather than specific times) are reported for each peak in the data tables. In some samples, closely eluting peaks did not resolve but coalesced into a single peak range. In such cases, the reported peak area pertained to the group of peaks expected in the time interval in question. Given the inherently low resolution of the detection system, it is possible that some of the identified peaks may contain more than one

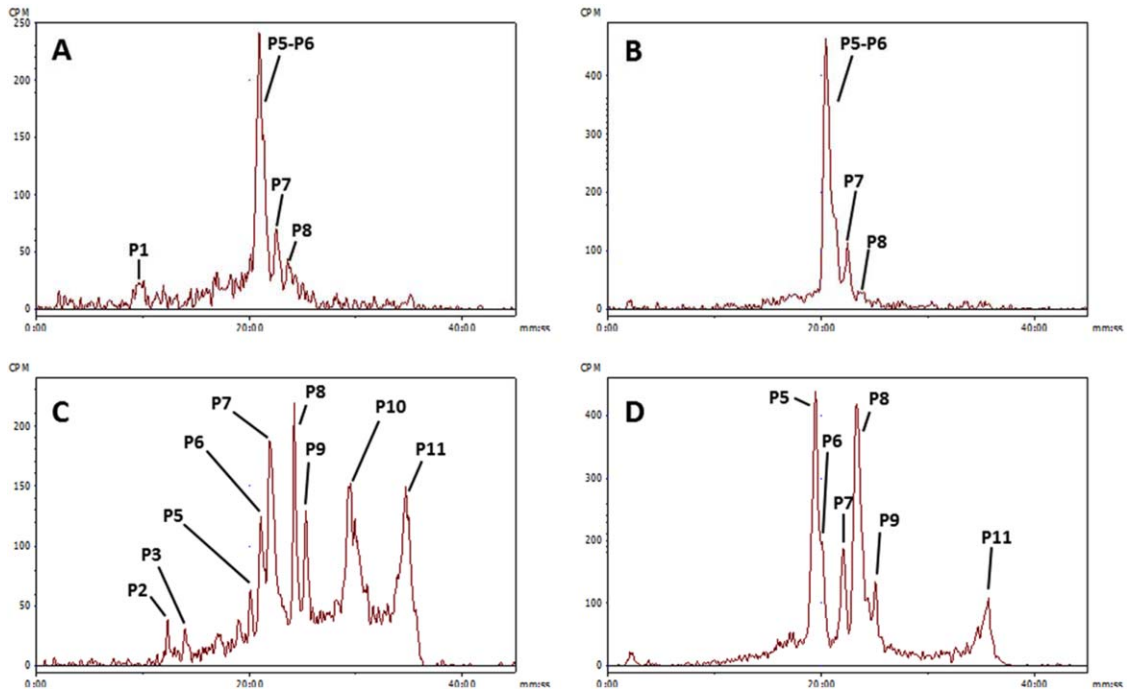

Fig. 6. Representative radio-chromatograms of excreta after administration of [^{14}C]-3,4,3-LI(1,2-HOPO) to rats. A: urine of a male animal at 8 h; B: urine of a female animal spiked with [^{14}C]-3,4,3-LI(1,2-HOPO); C: feces of a male animal at 24 h; D: feces of a male animal at 8 h spiked with [^{14}C]-3,4,3-LI(1,2-HOPO). [Color figure can be viewed in the online issue, which is available at wileyonlinelibrary.com.]

species. The relative percent peak area was normalized to the percent of the administered dose present in the tissue sample analyzed.

RESULTS

Pharmacokinetic parameters and disposition/biodistribution of [^{14}C]-3,4,3-LI(1,2-HOPO) were characterized in vivo in two separate studies using young adult Swiss Webster mice and Sprague Dawley rats. In the first study, groups of six mice (3 male, 3 female) were given a single dose via iv, ip, or po routes. In addition, one group was administered the ^{14}C-labeled API with permeability enhancer (API + PE) by po. At scheduled time points, blood, liver, kidney, and excreta were collected and analyzed for ^{14}C content using LSC. Similarly, in a second study, groups of six rats (3 male, 3 female) were administered a single iv dose of the ^{14}C-labeled API or a single po dose of the ^{14}C-labeled API + PE formulation. At scheduled time points, blood, brain, liver, kidney, lungs, spleen, and skeletal muscle tissues, GI tract samples, carcasses, and excreta were collected and analyzed as above. Unless stated otherwise, all values are reported based on radioactivity analysis. Tissue content is expressed in μg-eq, while excretion data are given as percentage of administered dose (% AD).

Uptake and Retention in Kidneys and Liver

Following an iv or ip injection of [^{14}C]-3,4,3-LI(1,2-HOPO), radioactivity was rapidly distributed into highly vascular tissues for both mice (Fig. 2, Panels A and C) and rats (Fig. 3, Panel A). The highest kidney concentrations were seen early, at 1 h after both iv and ip injection for the mouse cohorts and at 2 h after iv injection for the rat cohorts, with slightly higher maximum radioactivity levels in the kidney for rat (1643 and 576.4 μg-eq in males and females, respectively) compared to mice (up to 385.3 and 514.4 μg-eq in males and females, respectively) after iv injection. Comparison of the two parenteral administration routes in mice also indicated that the kidney had a higher ^{14}C content when the ligand was introduced into the body via iv versus ip. In contrast, the oral administration route resulted in minimal concentrations of API in kidney for both mouse (Fig. 2, Panel E) and rat (Fig. 3, Panel C) cohorts (9.0 and 0.6 μg-eq in male and female mice at 1 h and 45 min, respectively; 1.0 and 0.4 μg-eq in male and female rats, respectively, at 2 h). Finally, the distribution of [^{14}C]-3,4,3-LI(1,2-HOPO) in mouse kidney

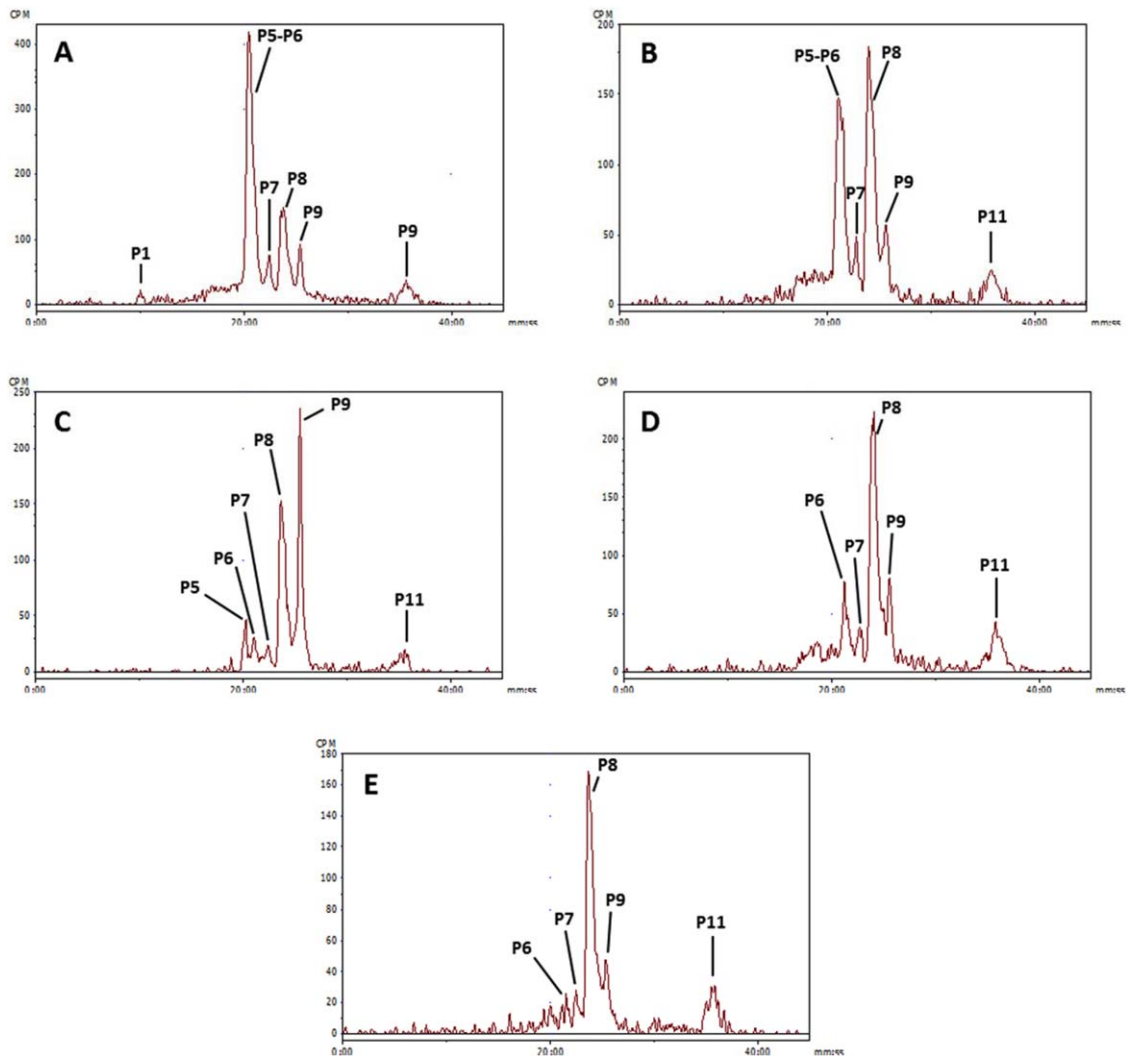

Fig. 7. Representative radio-chromatograms of tissue homogenates after administration of [^{14}C]-3,4,3-LI(1,2-HOPO) to rats. A: kidney homogenate from a male animal at 6 h; B: kidney homogenate from a female animal at 2 h spiked with [^{14}C]-3,4,3-LI(1,2-HOPO); C: liver homogenate of a female animal at 2 h; D: liver homogenate from a male animal at 2 h spiked with [^{14}C]-3,4,3-LI(1,2-HOPO); E: lung homogenate from a female animal at 2 hr. [Color figure can be viewed in the online issue, which is available at wileyonlinelibrary.com.]

appeared to be dependent on the route of administration and animal sex. Significantly, lower ($P < 0.05$) ^{14}C level was observed in kidneys of the male mice when compared to the females at 24 h post-ip dose. In contrast, consistently lower ^{14}C levels were found in the kidney of female mice starting at 1 h up to 24 h post po dose when compared to males that were treated orally ($P < 0.05$).

Similar to what was observed in kidney, the liver showed substantial levels of ^{14}C after a single iv or ip administration of [^{14}C]-3,4,3-LI(1,2-HOPO) in mice (Fig. 2, Panels A and C) and after a single iv administration in rats (Fig. 3, Panel A). Liver radioactivity levels were high and sustained after iv injection for both mice and rats, from the first sampling time point through 24 h. Slightly higher maximum ligand concentrations were observed for rats (up to 294.3 and 381.2 μg-eq in male and female, respectively) compared to mice (up to 236.6 and 151.0 μg-eq in male and female, respectively). Liver radioactivity levels stayed constant over the first 24 h post-injection for the rats, while it slowly decreased over time for the mice but was still detected in the organ even at 24 h post administration in notable amounts (39.9 and 44.1 μg-eq in male and female, respectively). A similar trend was observed in the female liver after an ip administration where there was a slight delay in reaching the liver compared to iv; nonetheless, a significant level of ^{14}C was detected by 15 minutes. Similar slow

decrease profiles but consistently lower amounts of ^{14}C were found in the liver from the ip route compared with the iv route in mice. In contrast, when the ligand was administered orally, only low radioactivity counts were recorded at all scheduled time points for both mouse (Fig. 2, Panel E) and rat (Fig. 3, Panel C) cohorts with a slightly higher liver uptake in male mice when compared with females.

Uptake and Retention in Other Tissues

As liver and kidney are the major sites of actinide deposition after contamination, these organs were the focus of the mouse studies. To investigate total body distribution, additional tissues were analyzed in the rat study, as depicted in Figure 3, Panels A and C. Relatively high levels of ^{14}C were found in the brain, lung, spleen, and skeletal muscle tissue at the first 2 h collection time point after iv injection (8.6, 176.4, 10.6, and 14.2 μg-eq, respectively for males and 9.7, 166.3, 19.3, and 5.0 μg-eq, respectively for females). However, the ^{14}C content gradually decreased over time in these tissues, confirming that the ligand does not persist at those sites. Minimal uptake followed by clearance in those same tissues was also observed after po administration. In contrast, large amounts of ^{14}C were detected in the GI tract samples and carcasses at the last 24 h time point after both iv and po administrations. The compound accumulation in the GI tract of iv-administered rats is most likely attributed to biliary excretion. This is confirmed by the increasing cumulative fecal ^{14}C levels over time. No obvious difference was observed between male and female animals.

Urinary and Fecal Excretion

Figures 2 and 3 show the cumulative urinary and fecal excretion patterns in mice (Panels B, D, and F) and rats (Panels B and D), respectively. The combined total excretion by 24 h was similar between male and female animals for each route of administration investigated, except for the mice administered the ligand by iv injection. The male mice in this treatment group excreted about half of the injected radioactivity when compared with the females (55.7% vs. 101.4% AD, respectively). Combined excretion at 24 h was higher in mice than in rats that were comparably treated. A 30–40% AD was found in both male and female rats in the iv group, while more than 85% AD was recovered in the excreta of orally treated male and female mice. The male mouse cohort eliminated a greater percentage of ^{14}C through the renal pathway than the female cohort after receiving an iv (22.0% vs. 12.3% in male and female, respectively) or ip dose. In contrast, the female rat cohort had a greater renal elimination than the corresponding male group after iv administration.

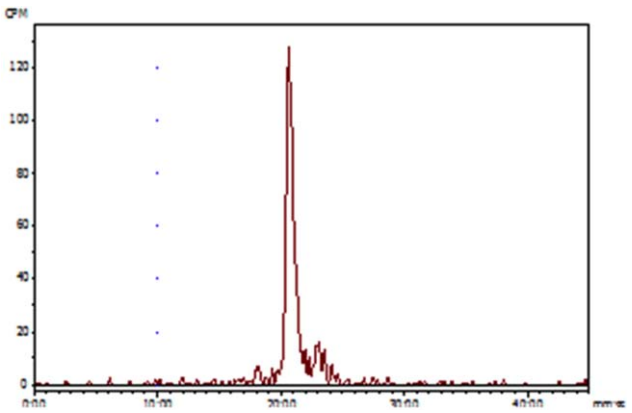

Fig. 8. Radio-chromatogram of the [^{14}C]-3,4,3-LI(1,2-HOPO) iv dose solution. The dose solution was diluted 32-fold in mobile phase A and injected as it is. [Color figure can be viewed in the online issue, which is available at wileyonlinelibrary.com.]

Compared to the parenteral routes, there was minimal urinary output of ^{14}C when the compound was given orally. In mice, the highest accumulation of ^{14}C was seen in the feces after all three administration routes, confirming that the biliary pathway is the main mode of elimination. A discrepancy was observed in the fecal output between male and female mouse cohorts, with exceedingly higher fecal radioactivities measured in females when the ligand was administered intravenously (34% in male compared to 89% in female). With the ip route, the percentage of ^{14}C output was comparable (37% and 44% in male and female mice, respectively). In contrast, elimination seemed to occur through both renal and biliary paths in rats after iv injection. However, when given orally, the ligand was removed from the body almost entirely through the fecal pathway.

Pharmacokinetics of [^{14}C]-3,4,3-LI(1,2-HOPO)

The mean ^{14}C concentrations in the plasma 5 min to 24 h after parenteral and oral administration are presented in Figure 4, Panels A, C, and E for mice and Panels B and D for rats. Plasma concentration-time profiles showed similar log-linear decays after iv administration in mice and rats, and the radiolabeled compound was rapidly distributed throughout the extracellular fluid space with higher peak concentrations and total plasma exposure in rats (C_0 = 463 and 422 μg-eq/mL, AUC = 354 and 211 h

TABLE 2. Percent Relative Abundance of [^{14}C]-3,4,3-LI(1,2-HOPO) Metabolite Levels found in Male and Female Sprague Dawley Rats

				Peak ID (Retention Time Range in min.)**												
Matrix	Route	Time (hr)	Animal Sex	P1 (8:57 –9:54)	P2 (12:16 –12:33)	P3 (13:54 –13:58)	P4 (16.59)	P5 (19:42 –20:26)	P6 (20:30 –21:27)	P7 (21:42 –22:46)	P8 (23:28 –24:21)	P9 (25:06 –25:35)	P10 (29:14 –29:53)	P11 (33:43 –35:47)	P5 – P9 + P11 Combined Abundance
Urine	iv	4	M							NA*					
			F	–	–	–	–	**64.0**		**36.0**	–	–	–	–	100
		8	M	6.95	–	–	–	**76.0**		17.1	–	–	–	–	93.1
			F	6.51	–	–	–	7.26	**71.6**	14.6	–	–	–	–	93.5
		12	M	8.42	–	–	–	**63.0**		16.3	12.3	–	–	–	91.6
			F	–	–	–	–	**67.6**		19.0	13.4	–	–	–	100
		24	M	12.8	–	–	–	**61.2**		16.0	10.0	–	–	–	87.2
			F	–	–	–	–	–	17.2	**32.9**	**33.6**	9.15	–	7.21	100
	po	24	M	–	–	–	–	–	–	**100**	–	–	–	–	100
			F							NA*					
Feces	iv	12	M	–	–	–	–	–	8.26	12.6	14.1	10.6	**25.7**	**28.8**	74.3
			F	–	–	–	–	–	8.31	13.7	14.3	11.6	**22.8**	**29.4**	77.2
		24	M	–	2.44	1.73	–	3.33	8.30	19.0	11.4	7.54	**25.1**	**21.2**	70.8
			F	–	–	–	–	–	6.05	16.2	8.33	5.33	**40.9**	**23.2**	59.1
	po	24	M	–	1.45	1.83	–	4.36	4.78	17.8	10.0	3.49	**34.6**	**21.6**	62.1
			F	–	1.62	2.34	–	4.97	6.70	**26.7**	6.99	7.54	**30.0**	13.2	66.1
Kidney	iv	2	M	–	–	–	3.86	**48.0**	13.8	8.23	12.7	7.47	–	5.87	96.1
			F	–	–	–	–	–	**32.7**	8.49	**32.1**	11.3	–	15.4	100
		6	M	1.43	–	–	–	**53.9**	–	8.33	**22.0**	7.52	–	6.83	98.6
			F	–	–	–	–	–	**40.8**	10.6	**27.9**	10.7	–	10.0	100
		24	M	–	–	–	–	–	**22.3**	16.6	**31.8**	**21.5**	–	7.75	100
			F	–	–	–	–	–	8.55	11.1	**39.5**	**25.2**	–	15.6	100
Liver	iv	2	M	–	–	–	–	16.0	4.76	5.34	**45.5**	**22.4**	–	6.01	100
			F	–	–	–	–	6.90	5.26	6.13	**38.1**	**36.9**	–	6.75	100
		6	M	–	–	–	–	1.83	3.75	8.37	**25.3**	**53.6**	–	7.09	100
			F	–	–	–	–	–	3.84	4.41	**35.0**	**47.1**	–	9.61	100
		24	M	–	–	–	–	–	–	**21.0**	–	**68.8**	–	10.2	100
			F	–	–	–	–	–	–	11.7	9.18	**64.4**	–	14.7	100
Lung	iv	2	M	–	–	–	–	–	–	7.45	**74.3**	10.6	–	7.72	100
			F	–	–	–	–	–	6.80	7.46	**57.4**	12.9	–	15.5	100

*NA: not available due to insufficient sample quantity.
**Values highlighted in bold are 20% or greater.

TABLE 3. Selected [^{14}C]-3,4,3-LI(1,2-HOPO) Metabolite Levels in Male and Female Sprague Dawley Rat Samples*

				Peak ID (Retention Time Range in min.)†					
Matrix	Route	Time (hr)	Sex	P1 (8:57 –9:54)	P2 (12:16 –12:33)	P3 (13:54 –13:58)	P4 (16.59)	P10 (29:14 –29:53)	P1 − P4 + P10 Combined Abundance
Urine	iv	4	M				NA**		
			F	–	–	–	–	–	–
		8	M	0.235	–	–	–	–	0.235
			F	0.397	–	–	–	–	0.397
		12	M	0.258	–	–	–	–	0.258
			F	–	–	–	–	–	–
		24	M	0.394	–	–	–	–	0.394
			F	–	–	–	–	–	–
	po	24	M	–	–	–	–	–	–
			F				NA**		
Feces	iv	12	M	–	–	–	–	4.16	4.16
			F	–	–	–	–	2.04	2.04
		24	M	–	0.241	0.171	–	2.47	2.88
			F	–	–	–	–	0.475	0.475
	po	24	M	–	0.435	0.549	–	**10.4**	**11.4**
			F	–	0.499	0.721	–	**9.24**	**10.5**
Kidney	iv	2	M	–	–	–	0.882	–	0.882
			F	–	–	–	–	–	–
		6	M	0.236	–	–	–	–	0.236
			F	–	–	–	–	–	–
		24	M	–	–	–	–	–	–
			F	–	–	–	–	–	–

*Expressed as percent of administered dose.
**NA: not available due to insufficient sample quantity.
†Values highlighted in bold are 5% or greater.

μg-eq/mL for male and female, respectively) than in mice ($C_0 = 76$ and 342 μg-eq/mL, AUC = 41.7 and 162 h μg-eq/mL for male and female, respectively), as reported in detail in Table 1. Intraperitoneal administration of [^{14}C]-3,4,3-LI(1,2-HOPO) in mice resulted in a lower level of radioactivity in plasma than through the iv route, but significantly higher ($P < 0.05$) than in the po route. The immediate exposure level of the ligand in plasma was slightly higher in female than male mice but the trend of the concentration-time curve was similar in all three routes. Conversely, the plasma levels after iv injections were slightly higher in male than female rats.

The oral bioavailability (F) of 3,4,3-LI(1,2-HOPO) is limited, as indicated by its low plasma exposure in male and female mice (Fig. 4, Panel C). Measured values showed that the F of the radioactive compound was slightly higher in females compared to males (1.2% vs. 2.6% in male and female mice, respectively; 0.4% vs. 1.2% in male and female rats, respectively), as shown in Table 1. To improve the oral bioavailability of this large octadentate chelator, the API (Active Pharmaceutical Ingredient) was coformulated with a proprietary excipient with permeability enhancement properties, resulting in a moderate improvement in systemic exposure (Fig. 5). The C_{max} improved by *ca*. 3-fold from 0.32 to 0.93 μg-eq/mL in male and 0.55 to 1.4 μg-eq/mL in female mice, when formulated with the PE. In addition, the AUC, when calculated over 2 h post-treatment, increased from 8.3 ± 6.2 to 17.4 ± 6.7 min μg-eq/mL in males and 23.0 ± 15.4 to 35.1 ± 18.9 min μg-eq/mL in females, which translates into an oral bioavailability improvement of approximately two-fold in mice. Based on these results, the coformulated API was used for oral administration in the rat study. The bioavailability of the mixture could not be compared to that of the API alone treatment as this group was not included in the rat study. Such comparisons are in progress and will be reported separately.

Metabolite Profiling

Samples from the rat biodistribution studies with the highest total radioactivity content were processed for metabolite profiling of [^{14}C]-3,4,3-LI(1,2-HOPO), leading to the analysis of selected urine

(at 4, 8, 12, and 24 h after iv administration and 24 h after po administration), feces (at 12 and 24 h after iv administration and 24 h after po administration), kidney (at 2, 6, and 24 h after iv administration), liver (at 2, 6, and 24 h after iv administration) and lung (at 2 h after iv administration) samples. Representative radio-chromatograms obtained from urine and feces (Fig. 6) and from kidney, liver, and lung (Fig. 7), as well as calculated relative abundances for each peak (Table 2) are reported. Despite some retention time (rt) variations between samples, recorded elution times were consistent across the majority of the samples. Retention times are reported as ranges and defined by the earliest and latest occurrence of each corresponding peak throughout all samples. Samples obtained by spiking parent [^{14}C]-3,4,3-LI(1,2-HOPO) into blank urine and blank homogenates of feces, kidneys, and liver were prepared to identify peaks that correspond to a direct interaction of [^{14}C]-3,4,3-LI(1,2-HOPO) with matrix constituents [e.g., complexes of 3,4,3-LI(1,2-HOPO) with metal ions] rather than through metabolic biotransformations of 3,4,3-LI(1,2-HOPO) (Panels B and D of Figs. 6 and 7). Inspection of all radio-chromatograms led to the identification of 11 peaks, designated P1–P11. Substantial profile similarities were observed across matrix, sex, collection time, and dose route. Peaks P5–P11 had the highest relative abundances across all samples (Table 2). However, peaks P5-P9 and P11 were also seen in blank matrices spiked with residual iv dose solution, albeit with different relative abundances. The residual iv dose solution showed no significant [^{14}C]-3,4,3-LI(1,2-HOPO) degradation when analyzed as neat compound (i.e., without being mixed with matrix, Fig 8). Therefore, peaks P5-P9 and P11 are neither metabolites nor degradations of the test article, but rather are likely products of an interaction between matrix constituents and the test article. These matrix interaction parent peaks represented 59.1–77.2% of the radioactivity in feces and 87.2–100% of the radioactivity in the other sample types (urine, kidney, liver, and lung). Conversely, the combined radioactivity levels of the potential metabolite peaks P1–P4 and P10 ranged from 22.8 to 40.9% in feces and from 0 to 12.8% in the other sample types. The most abundant potential metabolite peak P10 (rt from 29 min 14 s to 29 min 53 s) appeared only in feces. P10 levels in feces were *ca*. 10 times higher than that of any of the other potential metabolite peaks, accounting for 22.8–40.9% of the total radioactivity in feces. Peak P1 (rt from 8 min 57 s to 9 min 54 s) was the second most abundant potential metabolite species. P1 appeared in 4 out of 7 urine samples with a relative abundance of 6.5 to 12.8% and was also detected in one kidney sample at relative abundance of 1.4%. Peaks P2 (rt from 12 min 16 s to 12 min 33 s) and P3 (rt from 13 min 54 s to 13 min 58 s) were detected only in feces (3 of 6 samples), and had relative abundances ranging from 1.5 to 2.4%. Peak P4 (rt of 3 min 86 s) appeared only in one kidney sample at a relative abundance of 3.9%. Table 3 shows the levels of the potential metabolites (peaks P1-P4 and P10) expressed as a percent of the total radioactive dose administered. Although only a limited number of samples were tested, there was a trend toward significantly higher levels of potential metabolites in feces after po administration than after iv administration. In feces, species P10 was 9.2 to 10.4% compared with 0.5–4.2% of the administered po and iv dose, respectively, and species P2 and P3 were 0.4 to 0.7% compared with 0.2% of the administered po and iv dose, respectively. In urine, species P1 was the only peak not attributable to the test article, it represented 0.2 to 0.4% of the administered iv dose, and it was not present in the one po administration urine sample that was analyzed.

DISCUSSION

[^{14}C]-3,4,3-LI(1,2-HOPO) was distributed rapidly and profusely into the liver and kidney following an iv injection. In general, the highest level of radioactivity in kidney and liver was detected early: at 1 h in mice and 2 h in rats postdose. A similar trend was observed in mice injected ip, in which the highest level of radioactivity in kidney and liver of both sexes was detected at 1 h postdose. No major differences in the compound uptake into liver and kidney were observed between iv and ip routes of administration, indicating that both routes are effective for [^{14}C]-3,4,3-LI(1,2-HOPO) distribution. Radioactivity recovered in urine 24 h after iv and ip administration was similar, with a slightly increased output in male than female mice. Interestingly, more radioactivity was recovered in the feces of female mice when the compound was administered iv compared to ip.

Minimal levels of ^{14}C were detected in kidney after oral dosing. The liver samples showed higher levels of ^{14}C than the kidney throughout the course of the study. In addition, low and transient uptake was seen in rats for other analyzed tissues (brain, lungs, spleen, and skeletal muscle tissues). Overall, these results indicate that none of the analyzed tissues are sites of [^{14}C]-3,4,3-LI(1,2-HOPO) accumulation. In mice, fecal elimination accounted for approximately 61%, 40%, and 89% of the iv, ip, and po administered dose, respectively, suggesting that the biliary route is the predominant route of

elimination. There was no significant gender difference in the fecal excretion pattern in the ip or po route in mice. However, a difference in the fecal output between males and females was observed in the iv route, in which greater radioactivity was seen in the feces of the female mice. Renal excretion of ^{14}C began as early as 5 and 15 min after iv and ip injections, respectively. Furthermore, the male mice eliminated a greater percentage of ^{14}C through the renal pathway than the female mice after receiving an iv or ip dose (~23% in males after iv or ip dose compared with ~12% in females). No gender difference in the urinary output of ^{14}C was observed in the oral treatment mice, and only a slight amount of radioactivity (~1%) was renally excreted.

Lower but still predominant fecal excretion levels were observed in rats, with about 15% and 40% of the intravenously and orally administered doses, respectively, accumulated in the feces at 24 h. In contrast to what was observed in mice, the female rats eliminated a greater percentage of ^{14}C through the renal pathway than the males after receiving an iv dose (~12% in males compared with ~21% in females). Overall, for both mice and rats, male and female cohorts showed very similar trend in the uptake and retention of the orally administered API in plasma, kidney, liver, urine, and feces.

A limited quantity of [^{14}C]-3,4,3-LI(1,2-HOPO) was synthesized and made available for studies where male mice were dosed (iv and ip) at half the po level and radioactivity in the samples being readily detected by LSC despite the lower administered dose. In order to account for the difference in administered dose, excreta data were reported as percent of administered dose and radioactivity levels in plasma, kidney, and liver were reported as radioequivalent concentrations. One limitation of the biodistribution studies is that radioanalysis by LSC alone does not allow for the discrimination between the unaltered and structurally modified compounds. Metabolite profiling of [^{14}C]-3,4,3-LI(1,2-HOPO) was therefore performed on selected urine, feces, kidney, liver, and lung samples containing the highest total radioactive levels from the rat study. A total of 11 peaks were detected, of which 6 were assigned as originating from uncharacterized interactions between the test article and matrix components because they were also seen in spiked blank matrix controls. These 6 peaks are not metabolites and are considered alternate forms of the parent compound (e.g., complexes of the test article with metallic ions). The five other radioactive species are considered potential metabolites. Feces-specific metabolite peaks represented a combined 10.5–11.4% and 0.5–4.2% of the administered dose after po or iv administration, respectively. The most abundant peak represented up to 10% of the administered dose in feces after po administration while the other two feces-specific peaks represented less than 1% of the administered dose after po administration. This metabolite could be of biliary origin, or it could be the product of a transformation within the intestinal tract, either through a spontaneous degradation process or mediated by the intestinal flora, since it was not detected in liver samples. Only one metabolite peak was identified in urine, representing 0.4–0.2% of the administered dose after iv administration but absent after po administration, and was also seen in one kidney sample after iv administration. While few metabolites were observed in this analysis, it is clear that additional studies are required to characterize and confirm the identities of the measured ^{14}C and of the identified metabolites. Furthermore, a relatively small number of animals was used in both mouse and rat studies. A larger number of subjects would need to be investigated in order to make more decisive conclusions about gender differences in the uptake and retention of the compound.

Intravenous administration of DTPA is the only available approved chelating treatment to date. In the event of a mass casualty incident, it will be necessary to have available, an orally active chelating agent that can quickly reach the systemic circulation, effectively bind a broad spectrum of actinide metals, and can safely be removed from the body. Independent of the route of administration, radioactivity was detected early in the analyzed plasma and organs, indicating that 3,4,3-LI(1,2-HOPO) quickly reaches the systemic circulation and is distributed to the rest of the body. Low oral bioavailability is generally due to gut and/or hepatic first-pass metabolism, and/or limited absorption [Lipinski 2000; Lipinski et al., 2001]. Based on the colonic transit time in rats of 15.5 h [Enck et al., 1989], the radioactivity found in the feces in the first 24 h after po administration is most likely unabsorbed compound. Although hepatic metabolism followed by excretion in the bile is possible for 3,4,3-LI(1,2-HOPO) that is orally bioavailable, the very low level of radioactivity in the blood and tissues in the po group animals suggests that the predominant route of elimination of an oral dose of 3,4,3-LI(1,2-HOPO) is through the feces. Evaluation of the rat metabolite profiles demonstrated that a putative major metabolite of [^{14}C]-3,4,3-LI(1,2-HOPO) is formed that accounts for ~10% of an administered oral dose. Thus it is likely that the observed low bioavailability of [^{14}C]-3,4,3-LI(1,2-HOPO) is due both to biotransformation processes as well as relatively low

absorption after oral administration. Limited absorption may occur due to poor permeability across membranes and/or solubility. 3,4,3-LI(1,2-HOPO) is highly soluble in aqueous media (>75 mg/mL in water; clogP < -0.5). While good aqueous solubility is a desirable physicochemical property in drug development, it may also attribute to limited permeability of the compound to various biological barriers such as the intestinal epithelium [Hu and Li 2011]. It is plausible that the poor oral bioavailability of the ligand may be permeability-limited. The high number of ionizable groups, low Log P, a relatively large size of the molecule, and high polarity of the compound are all properties that contribute to this limited permeability, resulting in a passive membrane diffusion mechanism of action. By simply coformulated with the proprietary permeability enhancer, we noted that 3,4,3-LI(1,2-HOPO) quickly reached the systemic circulation (20 minutes after po administration), which is a highly desirable characteristic of a decorporating agent.

CONCLUSION

While this study demonstrates that [^{14}C] uptake in the kidney and liver was relatively similar between mice and rats, a difference was observed in the amount of [^{14}C] recovered in the feces between the two species investigated in both iv and po routes. Because no animal model can accurately predict the effectiveness of the test compound in humans, it is important that researchers consider different animal species and choose the most appropriate model for the drug they are developing. The ultimate goal of this project is to make available for the public an orally efficacious chelating agent that can enhance the removal of internalized actinides, thereby reducing the risks of long-term debilitating health effects. Plutonium, americium, and other actinide decorporation properties of 3,4,3-LI(1,2-HOPO) in rodents have been previously reported [Paquet et al., 2003]. However, it has not been confirmed whether the metals removed from the body are ligand bound or in free ion forms. Furthermore, excretion profiles of the male and female animals need to be better understood. Such studies are currently underway, and their results will be reported in due course.

ACKNOWLEDGMENTS

This work was supported by the National Institutes of Health/National Institute of Allergy and Infectious Diseases Medical Countermeasures Against Radiological Threats (MCART) Consortium (Contract #HHSN272201000046C to the University of Maryland School of Medicine), through the US Department of Energy under Contract #DE-AC02-05CH11231.

REFERENCES

Abergel RJ, Durbin PW, Kullgren B, Ebbe SN, Xu J, Chang PY, Bunin DI, Blakely EA, Bjornstad KA, Rosen CJ, et al. 2010. Biomimetic actinide chelators: an update on the preclinical development of the orally active hydroxypyridonate decorporation agents 3,4,3-LI(1,2-HOPO) and 5-LIO(Me-3,2-HOPO). Health Phys 99:401–407.

Abergel RJ, Raymond KN. 2011. Multidentate terephthalamidate and hydroxypyridonate ligands: Towards new orally active chelators. Hemoglobin 35:276–290.

Bunin DI, Chang PY, Doppalapudi RS, Riccio ES, An DD, Jarvis EE, Kullgren B, Abergel RJ. 2013. Efficacy and safety toxicology of hydroxypyridinonate actinide decorporation agents in rodents: Towards a safe and effective human dosing regimen. Rad Res 179:171–182.

Cassatt DR, Kaminski JM, Hatchett RJ, DiCarlo AL, Benjamin JM, Maidment BW. 2008. Medical countermeasures against nuclear threats: Radionuclide decorporation agents. Rad Res 170:540–548.

Cerveny TJ. 1989. Treatment of internal radionuclide contamination. In: Zajtchuk R, editor. Medical consequences of nuclear warfare. Falls Church, VA: TMM Publications, Office of the Surgeon General. p 56–68.

Durbin PW. 2006. Actinides in animals and man. In: Morss LR, Edelstein NM, Fuger J, editors. The chemistry of the actinide and transactinide elements. Netherlands: Springer p 3339–3440.

Durbin PW. 2008. Lauriston S. Taylor Lecture: the quest for therapeutic actinide chelators. Health Phys 95:465–492.

Durbin PW, Kullgren B, Xu J, Raymond KN, Henge-Napoli MH, Bailly T, Burgada R. 2003. Octadentate Hydroxypyridinonate (HOPO) ligands for plutonium (IV): Pharmacokinetics and oral efficacy. Radiat Prot Dosim 105:503–508.

Enck P, Merlin V, Erckenbrecht JF, Wienbeck M. 1989. Stress effects on gastrointestinal transit in the rat. Gut 30:455–459.

Gorden AEV, Xu J, Raymond KN, Durbin PW. 2003. The rational design of sequestering agents for plutonium and other actinide elements. Chem Rev 103:4207–4282.

Hu M, Li X. 2011. Barrier to oral bioavailability—an overview. In: Hu M, editor. Oral bioavailability: basic principles, advanced concepts, and applications. Wiley, Hoboken, NJ, USA.

Jarvis EE, An DD, Kullgren B, Abergel RJ. 2012. Significance of single variables in defining adequate animal models to assess the efficacy of new radionuclide decorporation agents: using the contamination dose as an example. Drug Dev Res 73:281–289.

Kullgren B, Jarvis EE, An DD, Abergel RJ. 2013. Actinide chelation: biodistribution and in vivo complex stability of the targeted metal ions. Toxicol Mech Methods 21:18–26.

Lipinski CA. 2000. Drug-like properties and the causes of poor solubility and poor permeability. J Pharmacol Toxicol Methods 44:235–249.

Lipinski CA, Lombardo F, Dominy BW, Feeny PJ. 2001. Experimental and computational approaches to estimate solubility and

permeability in drug discovery and development settings. Adv Drug Deliv Rev 46:3–26.

Paquet F, Chazel V, Houpert P, Guilmette R, Muggenburg B. 2003. Efficacy of 3,4,3-LI(1,2-HOPO) for decorporation of Pu, Am and U from rats injected intramuscularly with high-fired particles of MOX. Radiation Prot Dosim 105:521–525.

Rowland M, Tozer TM. 1995. Clinical Pharmacokinetics: Concepts and applications. Liipincott Williams and Wilkins, Baltimore, MD, USA.

US Food and Drug Administration. 2004. Guidance for Industry. Calcium DTPA and zinc DTPA drug products - submitting a new drug application, Silver Spring, MD, USA.

US Food and Drug Administration. 2006. Guidance for Industry. Internal radioactive contamination - development of decorporation agents, Silver Spring, MD, USA.

US Food and Drug Administration. 2009. Guidance for Industry. Animal models - essential elements to address efficacy under the animal rule, Silver Spring, MD, USA.